NOTES AND CORRESPONDENCE

The Effect of Radial Velocity Gridding Artifacts on Variationally Retrieved Vertical Velocities

SCOTT COLLIS AND ALAIN PROTAT

Centre for Australian Weather and Climate Research, Australian Bureau of Meteorology, Melbourne, Australia

KAO-SHEN CHUNG

Department of Atmospheric and Oceanic Sciences, McGill University, Montreal, Quebec, Canada

(Manuscript received 7 October 2009, in final form 22 March 2010)

ABSTRACT

This article investigates the source and impact of artifacts produced by ordered linear interpolation techniques on variationally retrieved updraft intensities. Qualitative reasoning for the generation of periodic perturbations in gridded products is presented, and a simple analytical investigation into the impact of gridding artifacts on updraft retrieval is carried out. By projecting a nonconvergent flow typical of Darwin, Australia, onto the viewing geometry of a scanning radar, a numerical assessment of the impact of gridding artifacts is carried out. A simple enhancement to ordered linear interpolation, mixed-order linear interpolation, is proposed to reduce gridding artifacts. Radial velocity grids produced using both techniques are used to investigate the generation of spurious updrafts, with the simple ordered linear interpolation technique producing erroneous updrafts on the order of 2 m s^{-1}. To investigate the impact on vertical velocities retrieved from a real weather event, radar-derived measurements taken during the active monsoon phase of Tropical Warm Pool International Cloud Experiment are gridded using both techniques, and vertical velocities are retrieved and contrasted.

1. Introduction

The retrieval of the three-dimensional wind field from multiple sets of radar-derived wind fields requires the interpolation of the data onto a common coordinate system. The Cartesian coordinates of zonal and meridional displacement from the radar and height above sea level are commonly used. There are two common approaches to achieving this; ordered linear interpolation (OLI; Mohr and Vaughan 1979) or methods that use a weighting function such as the Cressman (1959) or Barnes (1964) filters plus more sophisticated methods such as adaptive Barnes filters (Askelson et al. 2000). Trapp and Doswell III (2000) contrast the two approaches, concluding that OLI is better at retaining higher spatial frequencies at the cost of generating artifacts at the beam-separation wavelength. Cressman and Barnes filters suppress these artifacts, reducing higher-frequency spatial information. This article investigates the impact of these gridding artifacts on the retrieval of vertical velocities retrieved using a simple variational algorithm. Given the widespread use of OLI [e.g., in the Thunderstorm Identification, Tracking, Analysis and Nowcasting (TITAN; Dixon and Wiener 1993) set of utilities], and for brevity, this article will focus on OLI techniques only and neglect Cressman and Barnes filters.

2. Wind velocity retrievals from radar-derived radial velocities

The variational retrieval of wind velocity components from radial velocities (also referred to as variational multi-/dual-/single-Doppler analysis) involves the generation of a series of metrics (often referred to as cost functions) to be minimized, in this case using a conjugate gradient minimization algorithm. This technique was first used by Ray et al. (1980) for the study of tornadic

Corresponding author address: Scott Collis, Centre for Australian Weather and Climate Research, 700 Collins St., Melbourne, VIC 3001, Australia.
E-mail: scollis.acrf@gmail.com

DOI: 10.1175/2010JTECHA1402.1

storms and further developed in studies such as Testud and Chong (1983), Scialom and Lemaître (1990) and, most recently, Shapiro et al. (2009). The algorithm implemented for this study is based on work reported in Laroche and Zawadzki (1994) and later in Protat and Zawadzki (1999). Metrics used for retrievals presented in this study are 1) disagreement between measurements and projection of the retrieval (referred to as control, e.g., u, v, and w components of velocity) variables and 2) disagreement between the retrieved field and constraining models (smoothness and mass continuity). These metrics are simultaneously minimized to obtain a final retrieval. All terms are weak constraints. The measurement and continuity terms were weighted equally, while the weighting of the smoothness constraint was determined through trial and error.

Due to the geometry of the radar beams, measured radial velocities are predominantly a function of horizontal motions, so without a constraining model, namely, the anelastic mass continuity equation, robust retrieval of the vertical velocity component is not possible. The anelastic mass continuity equation can be expressed as

$$\frac{1}{\rho}\frac{\partial w'\rho}{\partial z} = -\nabla \cdot \mathbf{v}_h, \tag{1}$$

where w' is the model vertical velocity, ρ is mass density, $-\nabla \cdot \mathbf{v}_h$ is the convergence of the horizontal wind field, and z is height.

In practice the difference between the current guess for w and the modeled w' [with upward and downward integral height weighted as in Protat and Zawadzki (2000)] is minimized simultaneously along with the other metrics. However, to gain an appreciation for the effect of artifacts on the retrieved vertical velocities, let us consider w' in isolation. The horizontal wind field of a purely westerly flow is taken to be

$$\mathbf{v}_h = [u + A\sin(2\pi x/\lambda), 0], \tag{2}$$

where u is the background flow, and A and λ are the amplitude and wavelength of the perturbation induced in the retrieved horizontal flow due to gridding artifacts. The divergence is

$$\nabla \cdot \mathbf{v}_h = \frac{2\pi A}{\lambda}\cos(2\pi x/\lambda), \tag{3}$$

which reaches a maximum of $2\pi A/\lambda$. Expanding (1) at the positions of maximum divergence gives

$$w'\frac{\partial \rho}{\partial z} + \rho\frac{\partial w'}{\partial z} = -\rho\frac{2\pi A}{\lambda}. \tag{4}$$

Discretizing (4) over a slab Δz of the atmosphere and solving for $\Delta w'$ yields

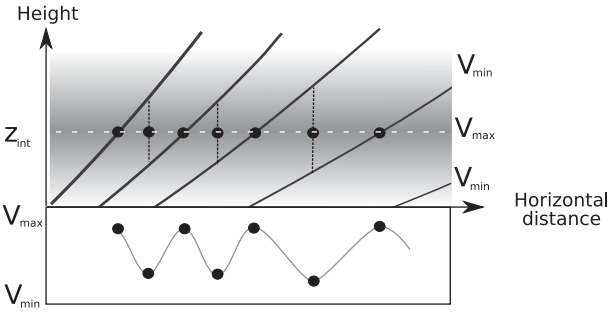

FIG. 1. An illustration showing the effect of a nonlinear gradient in radial velocity (represented by the gray gradient) on an interpolation of radar-based measurements as shown by the curve in the lower panel.

$$\Delta w' = -\frac{2\pi A}{\lambda}\Delta z + w'\frac{\Delta \rho}{\rho}. \tag{5}$$

Therefore, to first approximation, the perturbation on the model vertical velocity will be proportional to the product of amplitude and wavenumber ($1/\lambda$) of the perturbation on the horizontal flow field. As will be discussed in the next section, perturbations in the horizontal flow field arising from gridding artifacts can be on the order of 1 m s^{-1}, inducing (using this simple model) errors in the vertical velocity of a few meters per second.

3. Velocity gridding artifacts

Artifacts in interpolated data can arise when a linear interpolation method is used to grid measurements of nonlinear phenomena that are sparsely sampled in the direction of the nonlinearity. For example, radar-derived radial velocities where there exists a region of nonlinear gradients in velocity (e.g., over the maximum of a jet) at an elevation where there is a separation between the sampling beams. Figure 1 shows the propagation path of a series of radar beams in red. The background image represents a jetlike structure in westward-propagating winds as a gray gradient between $V_{\min}$ and $V_{\max}$, while the black dots represent a series of points (at height z_{int}) on which to be interpolated. The bottom figure shows the resultant radial velocity field derived using vertical interpolation. When the position of the desired interpolation is coincident with a radar beam the result is $V_{\max}$. Between the propagation paths it is a distance-weighted sum resulting in an interpolated value between $V_{\max}$ and $V_{\min}$. This causes undulations in the interpolated field where the wavelength is equal to the horizontal spacing of the radar beams at z_{int}, and the amplitude (A) is proportional to the gradient of the feature and horizontal spacing of the radar beams. This effect is also observed in gridded reflectivities in the vicinity of a bright band

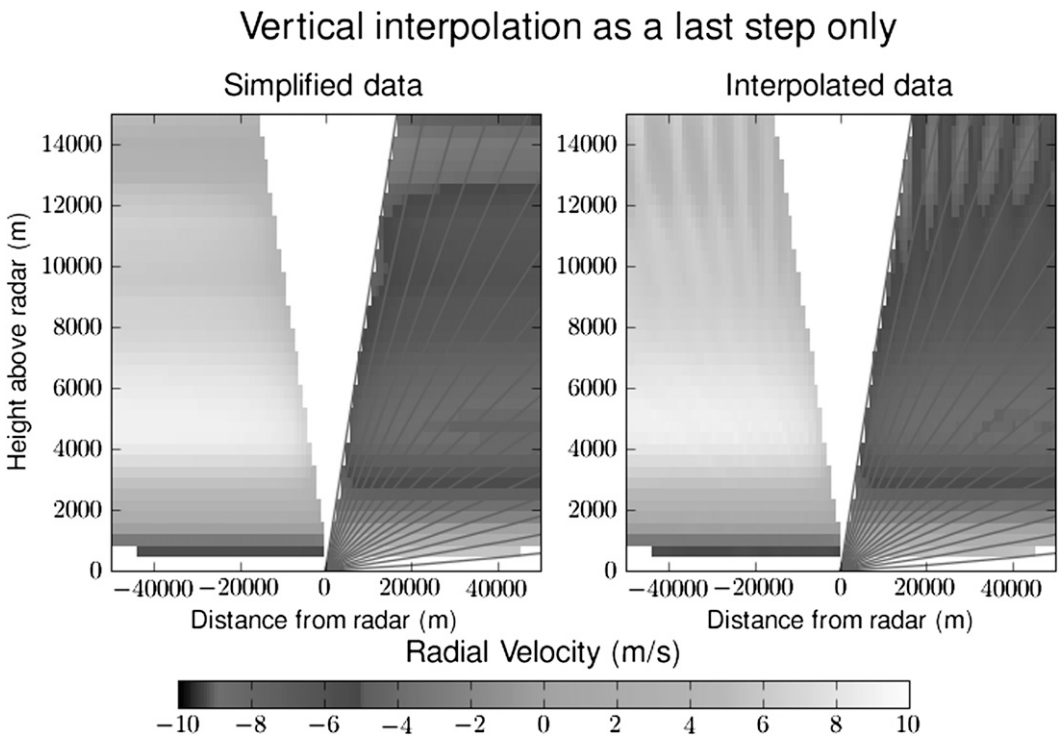

FIG. 2. (left) A synthesized radial velocity wind field (relative to C-POL) typical of the active monsoon flow in Darwin. (right) The result of projecting the wind field onto the viewing geometry of C-POL and gridding the synthesized measurement. Perturbations at the frequency of the beam propagation separation are shown (propagation paths are overplotted).

caused by the melting layer. To investigate the impact of velocity artifacts quantitatively, a simulated vertical profile of wind speed and direction was generated. The profile was typical of flow conditions over Darwin, Australia, during the active monsoon period of January 2006 [during the Tropical Warm Pool International Cloud Experiment (TWP-ICE; May et al. (2008)]. The radial component of the wind field [shown in Fig. 2 (left)] was calculated and projected onto the viewing geometry of a typical scanning strategy for the C-band polarimetric radar (C-POL; Keenan et al. 1998). The simulated radar measurements were then gridded using an OLI scheme (with the order of interpolation being range, azimuth, and then elevation, similar to that used in many operational systems). Figure 2 (right) shows the gridded data with the viewing geometry of C-POL overlaid. Perturbations in regions of high wind speed gradients at higher elevations are clearly evident. Figure 3 shows a profile of the regridded radial velocity where the radial velocity perturbations are greatest. The perturbations have a wavelength of 10 km and an amplitude of approximately 1 m s^{-1} over a vertical depth of 3 km. This yields a perturbation on the retrieved updraft of 1.8 m s^{-1}, which will have a significant impact on the ability to resolve subtle dynamical features.

4. Mixed-order ordered linear interpolation

Until now only OLI with the vertical interpolation as the last step has been discussed. Performing an OLI with the horizontal interpolation as the last step (interpolate in height, azimuth, and then radially) resolves the issue

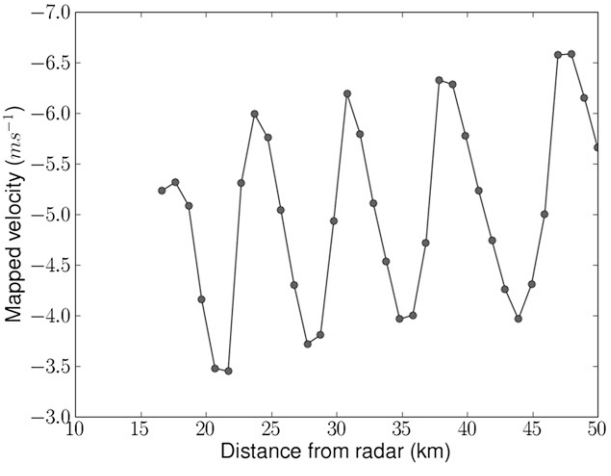

FIG. 3. A line plot of the gridded radial velocity data at 14 km showing, quantitatively, the gridding artifacts.

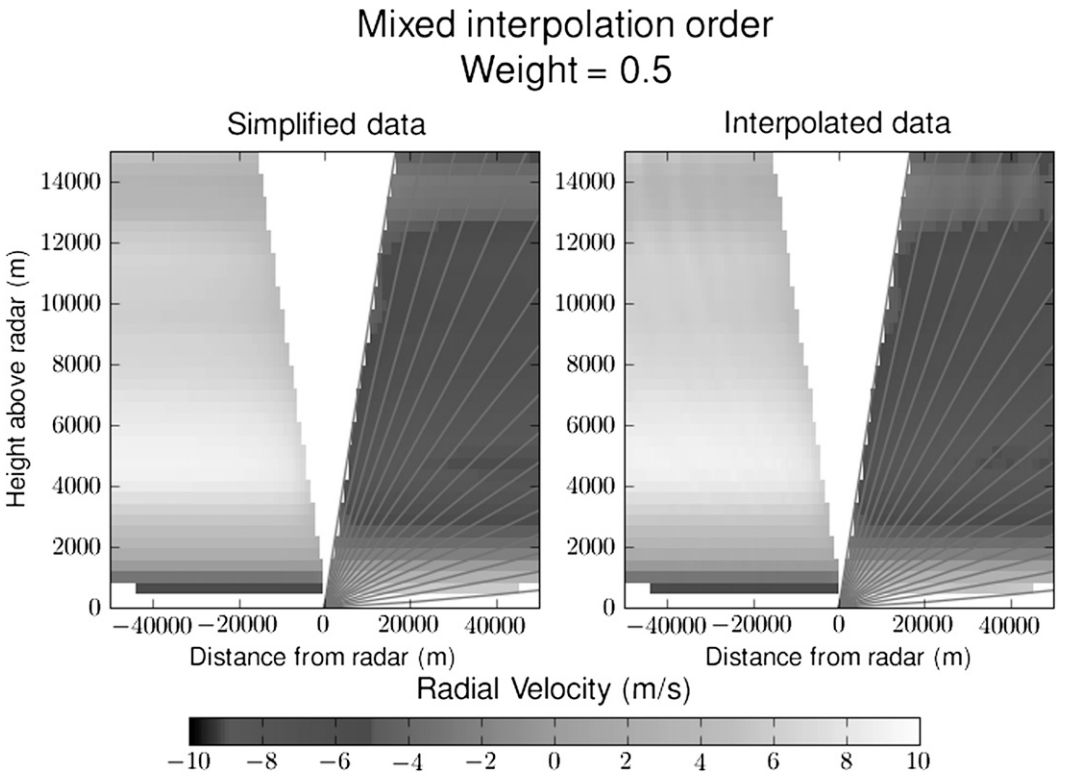

FIG. 4. (left) Synthesized wind field and (right) the interpolation using mixed order of interpolation of that wind field after projecting onto a standard radar scanning strategy.

of nonlinear shear features in the vertical inducing artifacts but results in very poor horizontal resolution (figure not shown). A trade-off is to do both a horizontal-last OLI and a vertical-last OLI and return a weighted sum of the two results, referred to as mixed-order ordered linear interpolation (MOLI). This is similar to the technique used by Zhang et al. (2005) to suppress brightband-induced rings in reflectivity mosaics. For illustrative purposes a simple weighting function w_h is used and is a function of the antenna elevation angle (corresponding to the point to be interpolated to) θ_e expressed as

$$w_h = \left[\frac{\sin(\pi\theta_e/\theta_{e,\max} - \pi/2) + 1}{2}\right]^n, \qquad (6)$$

where w_h is the weighting of the horizontal last OLI, $\theta_{e,\max}$ is the maximum antenna elevation, and n is the value that controls the shift from horizontal-last to vertical-last interpolation. The weighting for the vertical-last interpolation is simply $w_v = w_h - 1$. This weighting function was chosen to smoothly vary from 1 at $\theta_e = \theta_{e,\max}$ to zero at $\theta_e = 0$. Figure 4 shows data gridded using the same procedure as that used to produce Fig. 2, except a MOLI algorithm with a value for n of 0.5 was used (the value used in all subsequent MOLIs shown in this paper). A value of 0.5 was decided on after sensitivity studies showed that this value represented a good trade-off between reduction of artifacts and preservation of detail at higher elevations for our scanning strategy (θ_e = 0.5° to 42° with 17 tilts). This value, and the shape of the weighting function, will vary depending on the scanning strategy (beam spacing and maximum elevation). Different orders would be appropriate for differing scanning strategies and shear environments. Figure 5 shows the difference between the original and regridded field with the MOLI algorithm showing a reduction in the amplitude of gridding artifacts of around 0.5 m s^{-1}.

5. Impact on dynamic retrievals

To estimate the impact on updraft retrievals, the full variational retrieval must be performed. As in the last sections, a typical flow pattern observed in Darwin was projected onto the viewing geometry of the C-POL radar. In addition, these data were also projected onto the viewing geometry of the operational Berrimah Doppler radar, approximately 35 km to the southwest. The three-dimensional wind field was then retrieved for this laminar nonconvergent flow case using the retrieval technique outlined earlier. Figure 6 shows a vertical slice through

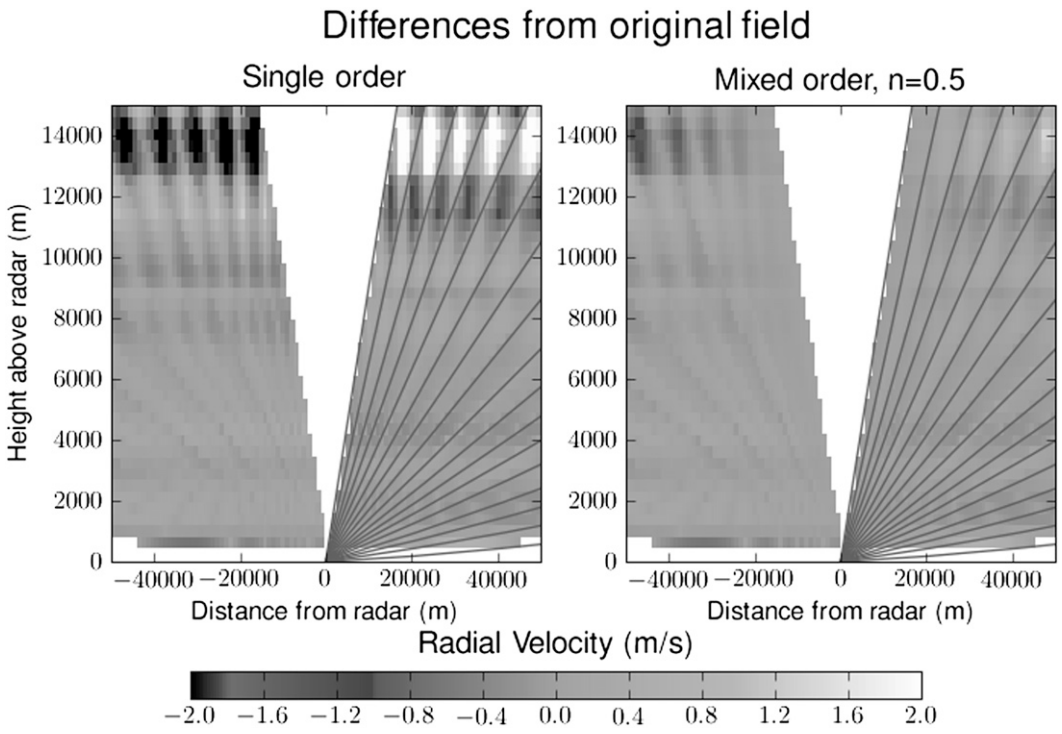

FIG. 5. Difference between the synthesized radial wind field and the interpolation of the projection of that wind field into radar coordinates using (left) a simple ''vertical last'' algorithm and (right) a mixed-order algorithm.

the regridded radial velocities as observed from the C-POL radar, with the vectors denoting the u and w components of the retrieved wind field overlaid. Single-order OLI (vertical last) is shown on the left, and the result of MOLI with order 0.5 is shown on the right. In the case of OLI, spurious updraft/downdraft pairs are reconstructed with vertical velocities of up to 5 m s^{-1}. The use of MOLI significantly reduces the magnitude of the spurious vertical velocities to less than 1.5 m s^{-1}.

One of the aims of TWP-ICE was to study the link between convective updrafts and the cloud properties of the resultant storm outflow. To produce updraft statistics for comparison with modeling studies [similar to that of Wu et al. (2009)], gridded data products must be free of artifacts that would cause spurious updrafts to be analyzed. To examine the impact of the artifacts highlighted in previous sections, a retrieval was performed on measurements from 8-min scans (the two radars, Berrimah and C-POL, were synchronized) starting at 1800 UTC 23 January 2006, during the active monsoon period of the field program. Data from both radars were mapped to a 100 km $\times$ 100 km $\times$ 25 km grid centered on the C-POL radar with a grid spacing of 1 km $\times$ 1 km $\times$ 0.5 km. Two grids were produced, one using OLI and the other using MOLI with order 0.5 (the same as the test case). Wind fields were then retrieved for both grids. Figure 7 shows a slice at constant latitude (at the latitude of the C-POL radar) through grids of horizontal reflectivity and retrieved wind fields. The u and w components of the winds are represented as arrows with the length being proportional to the wind speed. Data from grids produced using OLI are shown on the left while data produced from MOLI are shown on the right. There is a clear difference in the reflectivity images with the simple OLI producing more complexity in the vertical slice. The difference in the velocity vectors is not so clear until we compute the difference. Figure 8 shows the vector difference field (OLI minus MOLI). The grayscale background on the left shows the gridded radial velocity as produced by OLI, while the right-hand grid shows the radial velocity (with respect to CPOL) field produced using MOLI. There is a region of high outgoing radial velocities at 6-km altitude peaking around 18 m s^{-1}. In the case of OLI, clear fluctuations in the radial velocity can be seen just above the jet, while the blending of the horizontal last interpolation in the MOLI-produced grids suppresses the fluctuation. As can be seen in the difference vector field, the convergence/divergence associated with the fluctuation induces an updraft/downdraft pair of approximately 5 and -7 m s^{-1} in the retrieved wind fields. Because the radial velocity perturbation is periodic in nature and localized in vertical extent, it can be assumed

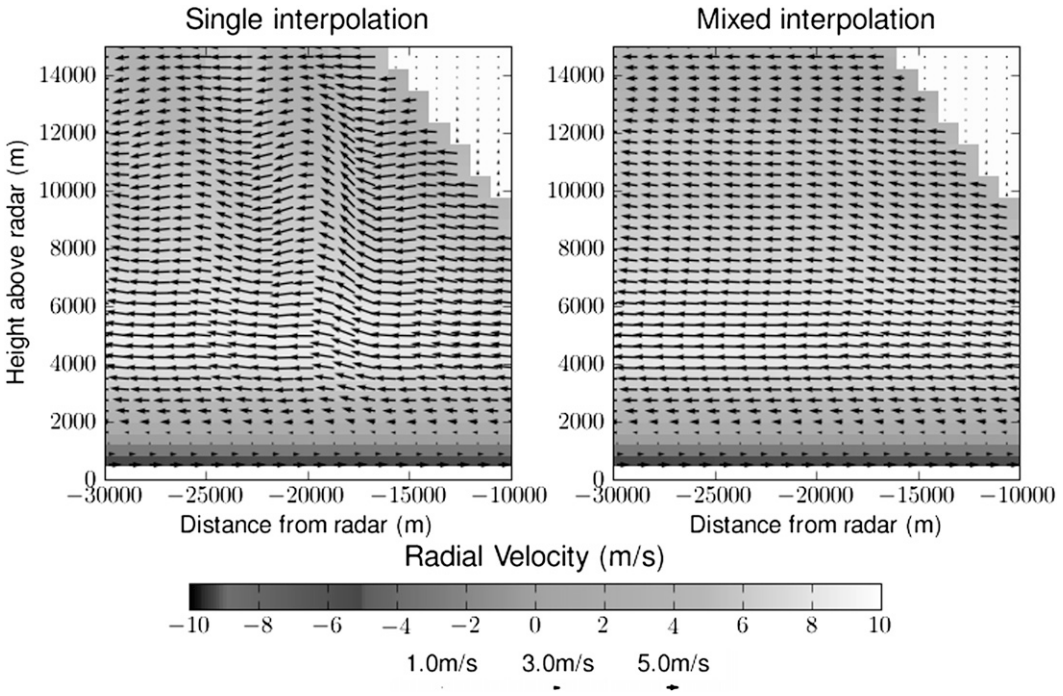

FIG. 6. The *u* and *w* components (vectors) of the variationally retrieved wind velocity fields from the grids produced using (left) OLI and (right) MOLI.

that it is a gridding artifact and that the associated updraft is spurious. A systematic error of this magnitude (on the order of retrieved updrafts) would produce a significant error in the computation of any storm statistics and complicate the elucidation of physical information. This provides a real-weather example of where a nonlinear-vertical-gradient-induced horizontal perturbation produces a nonexistent updraft. Therefore, care must be

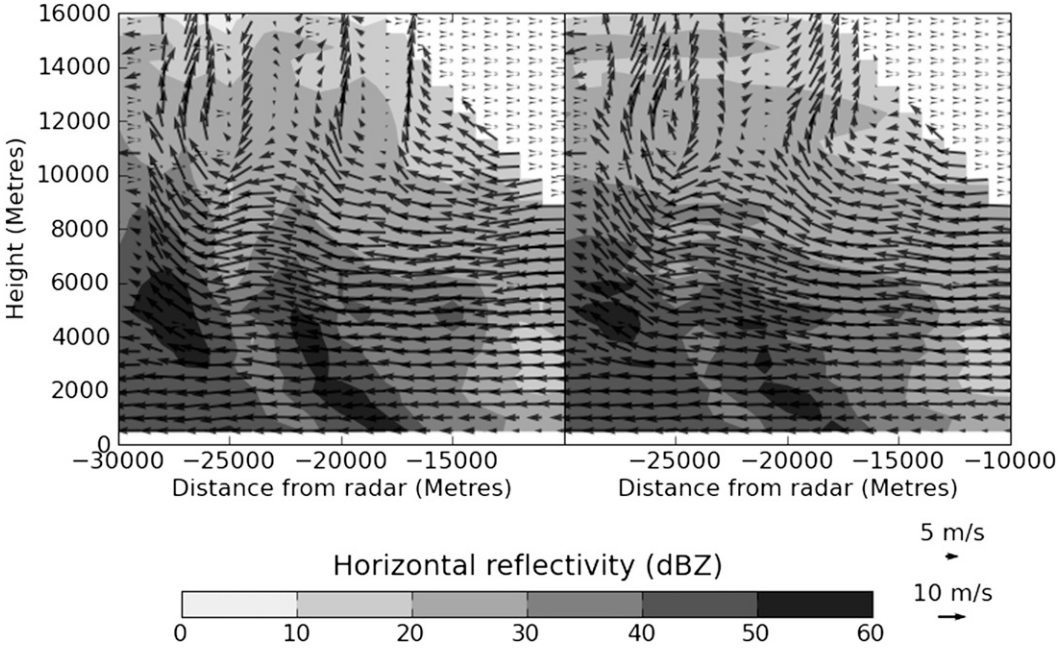

FIG. 7. A vertical cross section at a constant latitude through radar reflectivity measurements (grayscale background) and the *u* and *w* components of the variationally retrieved wind velocity fields: (left) results from using OLI and (right) results from MOLI.

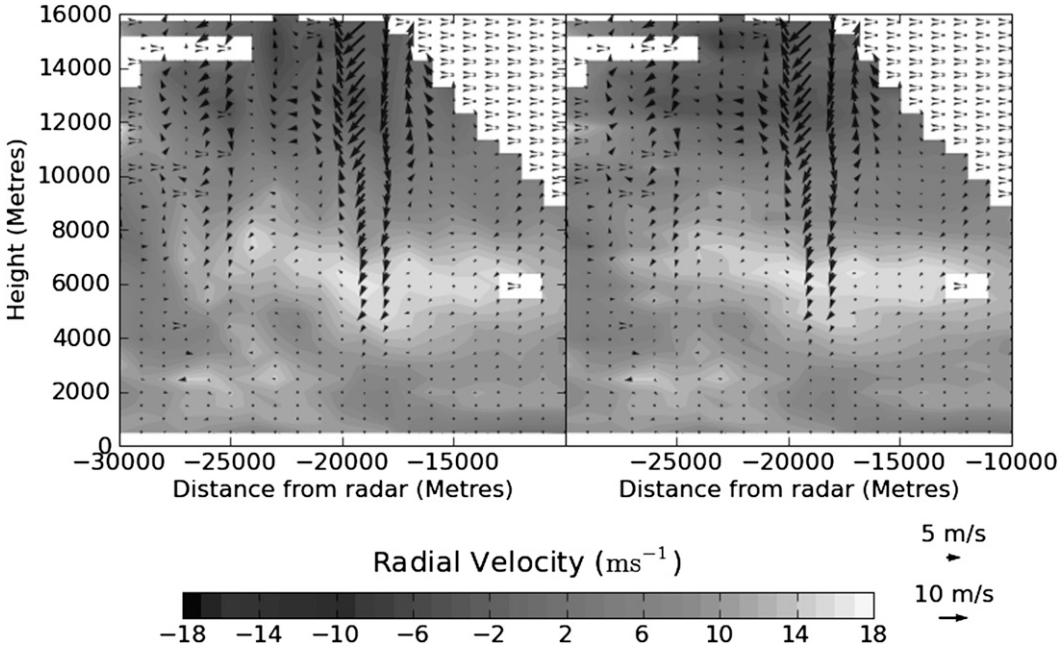

FIG. 8. As in Fig. 7, but with the gridded radial velocities as the grayscale background [(left) OLI; (right) (MOLI)] and a vector plot showing the *u* and *w* components of the difference between the winds retrieved from the OLI and MOLI grids (same for both grids: downward-pointing vector implies greater vertical velocities as a result of MOLI).

taken when using simple OLI techniques to produce grids to be used in variational velocity retrieval algorithms that use the anelastic mass continuity equation (or any other model using a spatial derivative) as a constraining model.

6. Conclusions

This article has shown the impact that gridding artifacts of the type discussed in Trapp and Doswell III (2000) have on winds retrieved using a variational algorithm. By taking a wind profile typical of the active monsoon over Darwin, Australia, and projecting it onto the viewing geometry of the C-POL radar, we found that nonlinear vertical gradients in tandem with the beam spacing produced perturbations in the ordered linear interpolation (OLI) of radial wind field of order 1 m s^{-1} with a wavelength of 10 km over a depth of approximately 3 km. Given a continuity cost of zero (i.e., the retrieved vertical velocities exactly match those calculated by integrating the anelastic mass continuity equation), these perturbations will induce spurious 1.8 m s^{-1} updrafts. This calculation is verified by using a variational retrieval technique similar to that described in Protat and Zawadzki (1999). A simple alternative to OLI is proposed that involves blending two linear interpolations tending to a horizontal-step-last scheme at high elevations and vertical step last at low elevations. This scheme suppresses gridding artifacts at the cost of reduced horizontal resolution at higher elevations. The article concludes by showing a real weather example where gridding artifacts are observed near a region of nonlinear vertical gradient in the radial wind field, resulting in the driving of a significant (5 m s^{-1}) spurious updraft. To find an ideal technique for gridding scanning radar products for the purposes of assimilation, Cressman and Barnes schemes also need to be considered. In addition, the effect of blending/estimating on suppressing real updrafts that occur on small scales must be investigated. This requires an independent measure of vertical velocity, either in situ or a nonscanning (e.g., vertical-pointing cloud radar/profiler) measurement. In the formulation of a robust system both these issues will be addressed in further studies.

Acknowledgments. This work has been partly supported by the U.S. Department of Energy Atmospheric Radiation Measurement (ARM) Program. We also wish to thank Peter May and Rodney Potts for their help in preparing this manuscript as well as the three anonymous reviewers for their insightful comments.

REFERENCES

Askelson, M. A., J.-P. Aubagnac, and J. M. Straka, 2000: An adaptation of the Barnes filter applied to the objective analysis of radar data. *Mon. Wea. Rev.,* **128,** 3050–3082.

Barnes, S. L., 1964: A technique for maximizing details in numerical weather map analysis. *J. Appl. Meteor.,* **3,** 396–409.

Cressman, G. P., 1959: An operational objective analysis system. *Mon. Wea. Rev.,* **87,** 367–374.

Dixon, M., and G. Wiener, 1993: Titan: Thunderstorm identification, tracking, analysis, and nowcasting a radar-based methodology. *J. Atmos. Oceanic Technol.,* **10,** 785–797.

Keenan, T., K. Glasson, F. Cummings, T. S. Bird, J. Keeler, and J. Lutz, 1998: The BMRC/NCAR C-band polarimetric (C-POL) radar system. *J. Atmos. Oceanic Technol.,* **15,** 871–886.

Laroche, S., and I. Zawadzki, 1994: A variational analysis method for retrieval of three-dimensional wind field from single-doppler radar data. *J. Atmos. Sci.,* **51,** 2664–2682.

May, P. T., J. H. Mather, G. Vaughan, C. Jakob, G. M. McFarquhar, K. N. Bower, and G. G. Mace, 2008: The Tropical Warm Pool International Cloud Experiment. *Bull. Amer. Meteor. Soc.,* **89,** 629–645.

Mohr, C. G., and R. L. Vaughan, 1979: An economical procedure for Cartesian interpolation and display of reflectivity factor data in three dimensions. *J. Appl. Meteor.,* **18,** 661–670.

Protat, A., and I. Zawadzki, 1999: A variational method for real-time retrieval of three-dimensional wind field from multiple-Doppler bistatic radar network data. *J. Atmos. Oceanic Technol.,* **16,** 432–449.

——, and ——, 2000: Optimization of dynamic retrievals from a multiple-Doppler radar network. *J. Atmos. Oceanic Technol.,* **17,** 753–760.

Ray, P. S., C. L. Ziegler, W. Bumgarner, and R. J. Serafin, 1980: Single- and multiple-Doppler radar observations of tornadic storms. *Mon. Wea. Rev.,* **108,** 1607–1625.

Scialom, G., and Y. Lemaître, 1990: A new analysis for the retrieval of three-dimensional mesoscale wind fields from multiple Doppler radar. *J. Atmos. Oceanic Technol.,* **7,** 640–665.

Shapiro, A., C. K. Potvin, and J. Gao, 2009: Use of a vertical vorticity equation in variational dual-Doppler wind analysis. *J. Atmos. Oceanic Technol.,* **26,** 2089–2106.

Testud, J., and M. Chong, 1983: Three-dimensional wind field analysis from dual-Doppler radar data. Part I: Filtering, interpolating and differentiating the raw data. *J. Appl. Meteorol.,* **22,** 1204–1215.

Trapp, R. J., and C. A. Doswell, III, 2000: Radar and objective analysis. *J. Atmos. Oceanic Technol.,* **17,** 105–120.

Wu, J., A. D. Del Genio, M.-S. Yao, and A. B. Wolf, 2009: WRF and GISS SCM simulations of convective updraft properties during TWP-ICE. *J. Geophys. Res.,* **114,** D04206, doi:10.1029/2008JD010851.

Zhang, J., K. Howard, and J. J. Gourley, 2005: Constructing three-dimensional multiple-radar reflectivity mosaics: Examples of convective storms and stratiform rain echoes. *J. Atmos. Oceanic Technol.,* **22,** 30–42.